ELSEVIER

Chemistry & Biology 8 (2001) 843–855

Chemistry & Biology

www.elsevier.com/locate/chembiol

Research Paper

The relationship between Taxol and (+)-discodermolide: synthetic analogs and modeling studies

Laura A. Martello [a], Matthew J. LaMarche [b], Lifeng He [a], Thomas J. Beauchamp [b], Amos B. Smith III [b,*], Susan Band Horwitz [a,1]

[a] *Department of Molecular Pharmacology, Albert Einstein College of Medicine, Bronx, NY 10461, USA*
[b] *Department of Chemistry, University of Pennsylvania, Philadelphia, PA 19104, USA*

Received 8 January 2001; revisions requested 27 February 2001; revisions received 12 June 2001; accepted 14 June 2001
First published online 11 July 2001

Abstract

Background: During the past decade, Taxol has assumed an important role in cancer chemotherapy. The search for novel compounds with a mechanism of action similar to that of Taxol, but with greater efficacy particularly in Taxol-resistant cells, has led to the isolation of new natural products. One such compound, (+)-discodermolide, although structurally distinct from Taxol, has a similar ability to stabilize microtubules. In addition, (+)-discodermolide is active in Taxol-resistant cell lines that overexpress P-glycoprotein, the multidrug-resistant transporter. Interestingly, (+)-discodermolide demonstrates a profound enhancement of the initiation process of microtubule polymerization compared to Taxol.

Results: The synthesis of (+)-discodermolide analogs exploiting our highly efficient, triply convergent approach has permitted structure–activity relationship (SAR) studies. Small changes to the (+)-discodermolide structure resulted in a dramatic decrease in the ability of all four discodermolide analogs to initiate tubulin polymerization. Two of the analogs also demonstrated a decrease in total tubulin polymerization, while a change in the olefin geometry at the C8 position produced a significant decrease in cytotoxic activity.

Conclusions: The availability of (+)-discodermolide and the analogs, and the resultant SAR analysis, have permitted an exploration of the similarities and differences between (+)-discodermolide and Taxol. Docking of the X-ray/solution structure of (+)-discodermolide into the Taxol binding site of β-tubulin revealed two possible binding modes (models I and II). The preferred pharmacophore model (I), in which the C19 side chain of (+)-discodermolide matches with the C2 benzoyl group of Taxol and the δ-lactone ring of (+)-discodermolide overlays with the C13 side chain of Taxol, concurred with the results of the SAR analysis.

Keywords: Discodermolide; Microtubule; Pharmacophore; Taxol

1. Introduction

Microtubules are required for a host of normal cellular processes, most importantly mitosis and cell division. When such an essential structure and the related biological functions are disrupted, cells can no longer undergo a normal cell cycle and eventually will die. Microtubules have become a key target for cancer chemotherapeutic drugs with many diverse natural compounds targeting the tubulin/microtubule system. Taxol, isolated from the Pacific Yew tree, has activity against a variety of human carcinoma cell lines and has been approved for the treatment of human breast, ovarian, and lung carcinomas [1]. In vitro, Taxol induces microtubule assembly in the absence of GTP that is normally required for assembly [2]. The resultant microtubules are stable against depolymerizing conditions such as cold temperatures or the addition of Ca^{2+}. Thus, Taxol blocks cells in the mitotic phase of the cell cycle and causes microtubule bundling, ultimately leading to cell death [3–5]. Even at low concentrations, the drug has a major effect on the dynamic instability of microtubules, reducing the dynamics dramatically [6,7].

Other novel tubulin-stabilizing agents, such as the epothilones, eleutherobin, and (+)-discodermolide, have been identified (Fig. 1) [8–11]. These natural products have been

[1] Also corresponding author.

* Correspondence: Amos B. Smith.
E-mail addresses: smithab@sas.upenn.edu (A.B. Smith III), shorwitz@aecom.yu.edu (S.B. Horwitz).

1074-5521/01/$ – see front matter
PII: S1074-5521(01)00055-2

isolated from a *Myxobacterium* fermentation, a marine soft coral, and a marine sponge, respectively. The new compounds have a mechanism of action very similar to that of Taxol in that they promote the assembly of stable microtubules, and induce mitotic arrest and microtubule bundling in cells, although each with a unique potency. A number of structure–activity relationship (SAR) and modeling studies have been performed with Taxol, the epothilones, eleutherobin, and (+)-discodermolide in a search for a common pharmacophore model for these drugs [12–16]. In this report, we provide evidence that (+)-discodermolide fits into a common pharmacophore model.

Although (+)-discodermolide was isolated and originally identified as a potential immunosuppressive agent [17], further studies revealed that the target of (+)-discodermolide was the microtubule system [10,11]. When compared to Taxol, (+)-discodermolide was found to be more potent at nucleating tubulin assembly [10,18], at inducing microtubule bundles in MCF-7 cells [10], and to have a higher affinity for tubulin [10,18]. However in cells, (+)-discodermolide was less cytotoxic than Taxol [18,19]. Recently, we have reported that Taxol and (+)-discodermolide represent a synergistic drug combination in human carcinoma cell lines, and as such may comprise a useful chemotherapeutic drug combination [19].

Although (+)-discodermolide holds promise as a cancer chemotherapeutic agent, the scarcity of the natural product (0.002% w/w from frozen sponge) had precluded further development of this agent as a drug. It is therefore not surprising that discodermolide has attracted considerable interest from the synthetic community resulting in seven total syntheses [20–26]. This includes our first-generation *ent*-discodermolide synthesis followed by a second-generation gram-scale synthesis of the natural isomer (+)-discodermolide [21,25]. In addition, two groups have reported the synthesis of analogs, laying the groundwork for a more detailed SAR study [27,28]. SAR studies have been performed with Taxol [29], the epothilones [30,31], and eleutherobin [32], but to date no SAR analyses examining microtubule stability and cellular effects have been reported for (+)-discodermolide. The present study compares the activity of discodermolide with four new analogs (Fig. 1), both in vitro and in cells, thereby providing important new information on the structural requirements responsible for the unique nucleation activity and potency of (+)-discodermolide.

2. Results

2.1. Synthesis of discodermolide analogs using a triply convergent approach

From the synthetic perspective, the polyproprionate structure of (+)-discodermolide revealed *Z*-olefinic linkages at C8–C9, C13–C14 and C21–C22, in addition to the carbamate and δ-lactone moieties (Fig. 1). The C13–C14 trisubstituted *Z*-olefin in particular represented a significant synthetic challenge. Indeed, installation of this structural unit proved troublesome for all previous synthetic approaches. We reasoned that modification of the discodermolide structure via deletion of the C14 methyl group, generating a *Z*-disubstituted olefin instead of the *Z*-trisubstituted olefin at C13–C14, would not only simplify the structure of the natural product, but also prospective synthetic strategies while retaining the biological activity. Support for the latter conjecture derives from the work of Hung et al., who reported that deletion of the C16 methyl group resulted in little or no loss of activity [27]. However, the group observed that changes in the C17–C20 region of the discodermolide backbone resulted in almost complete loss of activity [27]. Our focus thus turned to modification of the C1–C14 region of discodermolide with particular interest in the C14-normethyl analog (**2**). Ideally suited for this synthetic venture was our triply convergent synthetic approach to (+)-discodermolide [25,33]. In addition, a late stage Wittig olefination to install a variety of C1–C8 structure motifs would permit exploration, for the first time, of the SARs in this region.

The construction of other potentially important C1–C14 analogs also would be feasible due to the availability of significant quantities of several advanced intermediates. For example, in the late stage Wittig olefination leading to discodermolide (Scheme 1), we observed high selectivity (24:1 *Z*/*E*) favoring the *Z*-olefin **7** (69% yield); **7** was subsequently carried on to (+)-discodermolide (86%, three steps). To probe the importance of the olefin geometry at C8–C9, the minor *E*-olefinic isomer also was subjected to the same end game strategy. Oxidative removal of the paramethoxybenzyl (PMB) group with DDQ afforded the corresponding alcohol (52% yield), which was then subjected to the Kocovsky protocol to install the carbamate [34]. Global desilylation furnished the C(8, 9) *E* analog (−)-**4** in good yield (95%, two steps).

Another minor byproduct resulting from our gram-scale synthesis arose during the final global deprotection (i.e. **7**→(+)-discodermolide). Although the acidic conditions (3 N HCl, MeOH) led to the natural product reliably and in good yield (93%), the minor byproduct available due to the large scale synthesis proved to be the α,β-unsaturated δ-lactone (+)-**1**, obtained after purification by high performance liquid chromatography and recrystallization (CH_3CN); the structure was secured by single crystal X-ray analysis.

To probe further the substituents necessary for activity along the C1–C8 backbone, we sought several deletion analogs. Having developed a reliable route to terminal olefin (+)-**8** (Scheme 2) during the optimization of (−)-**6** [33], synthesis of an analog deoxygenated at C7 appeared feasible. Hydroboration of the terminal olefin using the

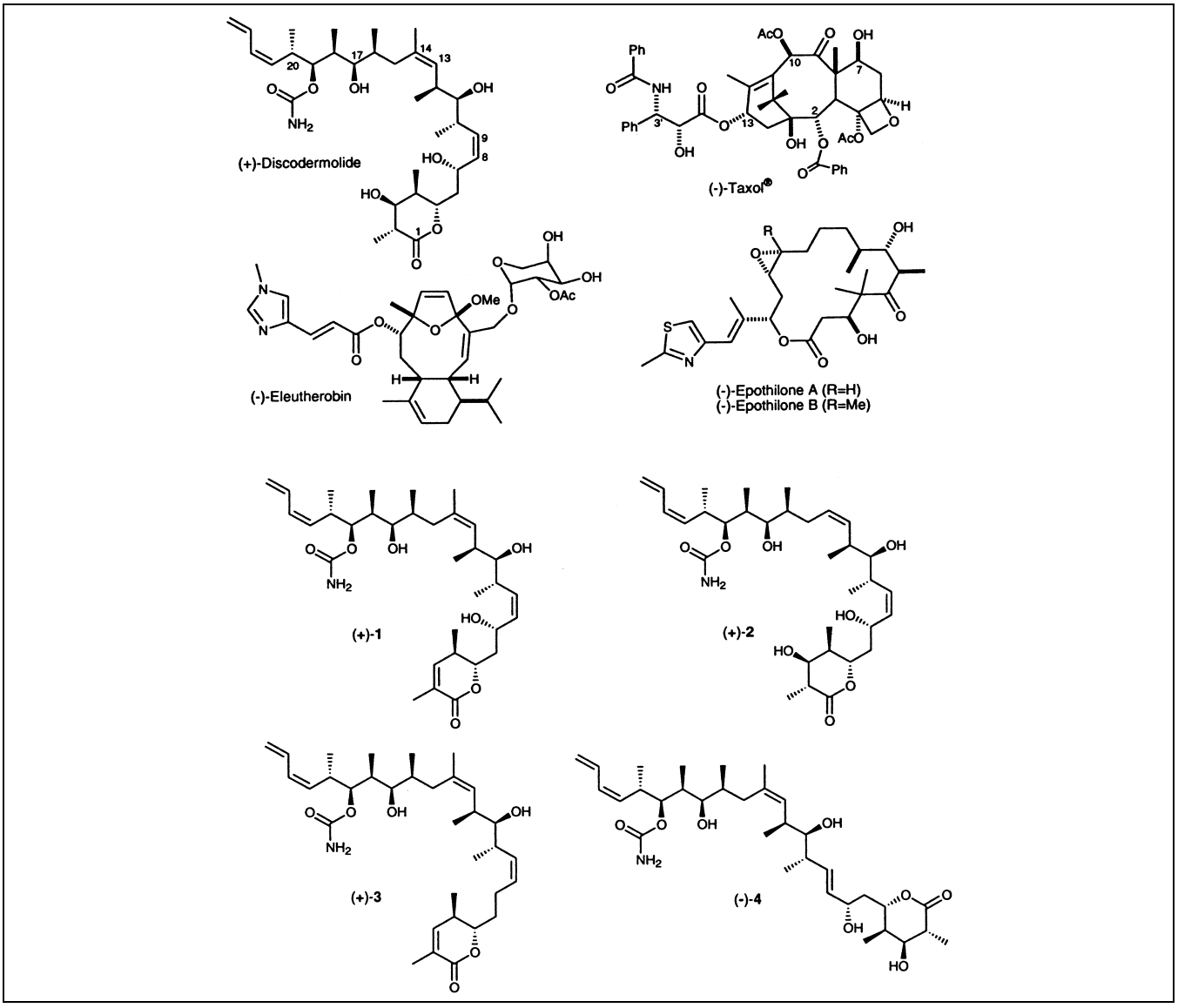

Fig. 1. Chemical structures of Taxol, the epothilones, eleutherobin, (+)-discodermolide, and discodermolide analogs **1–4**.

Evans protocol [35] provided alcohol (−)-**9** (70%); Parikh–Doering oxidation [36] then furnished aldehyde (−)-**10** (80%). Although Wittig olefination (Scheme 1) resulted in a modest yield (8%) of the *Z*-olefin **11**, we were able to complete the synthesis of the C7 deoxygenated analog. Towards this end, removal of the PMB group (DDQ, H_2O, 99%) followed by installation of the carbamate via the Kocovsky protocol furnished the carbamate. Surprisingly, treatment of the carbamate, as in our large scale synthesis of (+)-discodermolide (e.g. 3 N HCl, MeOH), led to (+)-**3**, the α,β-unsaturated δ-lactone as the major product (56%, two steps). Presumably the dehydration occurs in this case as a result of subtle conformational changes induced by deoxygenation at C7.

Our attention next turned to construction of the C14-normethyl analog of discodermolide (+)-**2** possessing a C8–C9 *Z*-olefin. As in our large scale discodermolide syntheses, we envisioned a Wittig reaction to introduce the *Z*-olefin linkage. In the earlier discodermolide syntheses, several groups [21,22] observed that the vigorous conditions required to generate the phosphonium salt **5** (Scheme 1) resulted in an undesired intramolecular cyclization involving the C13–C14 trisubstituted olefin. Generation of the Wittig salt at high pressure circumvented this problem [33]. We reasoned that replacement of the trisubstituted olefin with a *cis*-disubstituted olefin would in all likelihood negate the need for high pressure and thereby significantly simplify the overall synthetic strategy.

Our point of departure for the C14-normethyl analog (+)-**2** entailed a Stork–Zhao olefination [37] of aldehyde (−)-**12** [33] (Scheme 3) to furnish vinyl iodide (+)-**13** (13:1 *Z*/*E*; 73%), which upon Negishi cross-coupling [38] with

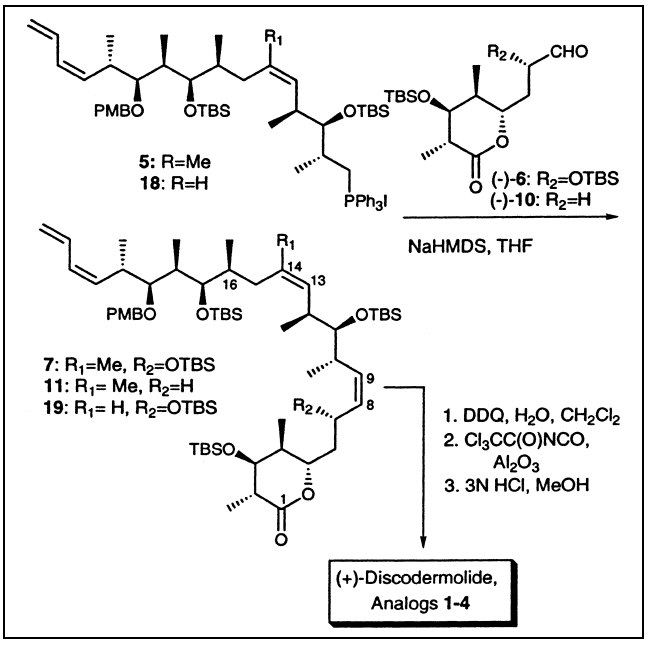

Scheme 1. Syntheses of (+)-discodermolide and analogs **1–4**.

our previously prepared iodide (+)-**14** [33] furnished olefin (+)-**15**. To facilitate the required discrimination of the C19 hydroxyl, we introduced a protecting group interchange. Specifically, the PMB group in (+)-**15** was removed chemoselectively (DDQ, H_2O, 80%) and replaced with a trityl moiety (tritylchloride, DMAP, pyr. 81%) to provide (+)-**16**.

Installation of the C21–C24 terminal *Z*-diene (Scheme 3) began with reductive opening of acetal (+)-**16** with DIBAL [39] followed by Dess–Martin oxidation [40]. The resulting aldehyde was then subjected to the Yamamoto diene synthesis [41] to furnish **17** (10:1 *Z*/*E*) in 63% yield (two steps). Removal of the minor *E*-diene isomer was accomplished at a later stage of the synthesis as previously achieved in our discodermolide synthesis [33]. The trityl group was next removed [42] (chlorocatecholborane, 80%), followed by conversion of the resulting alcohol to the iodide (Ph_3P, I_2, PhH/Et_2O) [43,44] to set the stage for generation of the Wittig salt. Intermolecular displacement of the iodide via molten triphenylphosphine (Hunig's base, 85°C) furnished the phosphonium salt **18** in high yield (95%, two steps), without involvement of the C13–C14 olefin. Thus, removal of the C14 methyl group from discodermolide significantly simplifies the generation of the requisite phosphonium salt and thereby the overall synthetic sequence.

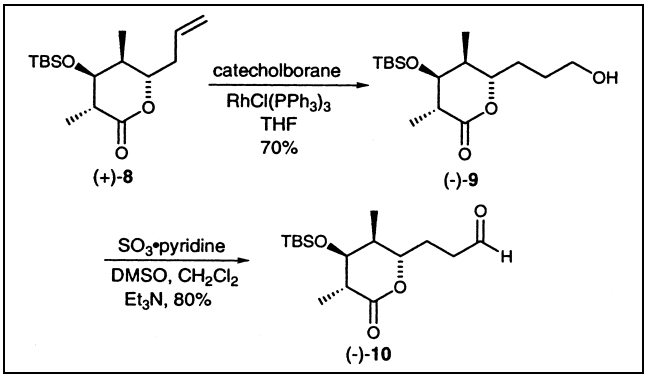

Scheme 2. Synthesis of modified C1–C8 coupling partner (−)-**10**.

Wittig coupling of the ylide **18** (Scheme 1) with aldehyde (−)-**6** [33] proceeded in 40% yield (7:1 *Z*/*E*) along with 35% recovery of the phosphonium salt which could be reused. Oxidative removal of the PMB moiety in **19** (DDQ, H_2O, 97%), installation of the carbamate via the Kocovsky protocol, and global deprotection (3 N HCl, MeOH; 89%) then furnished the C14-normethyl analog of discodermolide (+)-**2**.

2.2. Minor structural modifications of (+)-discodermolide result in a decrease in tubulin nucleation

The activities of Taxol, (+)-discodermolide, and the structural analogs were determined in an in vitro tubulin polymerization assay that measures changes in absorbance that correlate with the extent of microtubule polymerization. Microtubule polymerization involves both nucleation (initiation) and elongation steps. The initial rates of polymerization reflect the nucleation process [45]. Taxol, (+)-

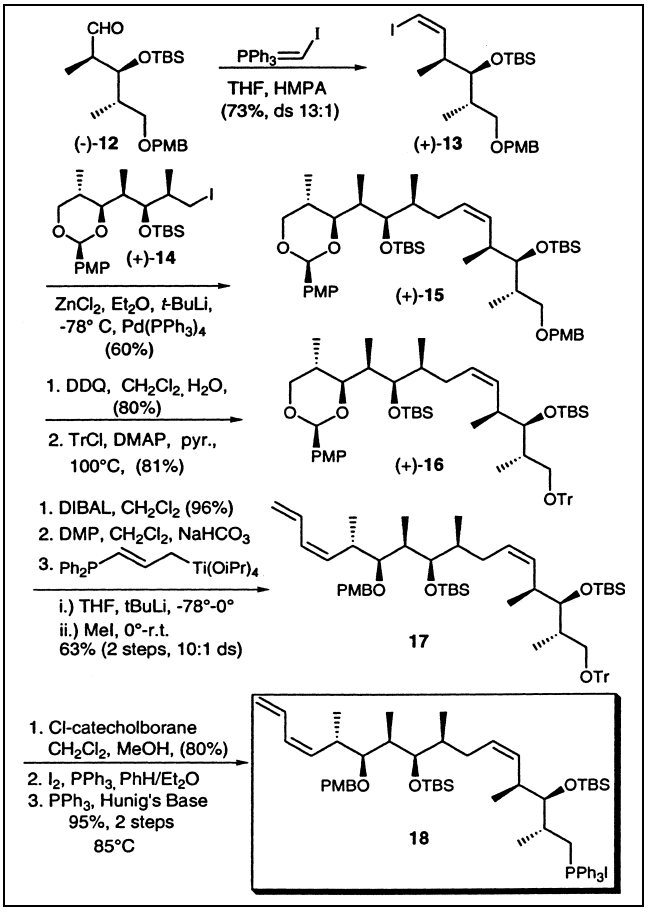

Scheme 3. Synthesis of C14-normethyl phosphonium salt **18**.

discodermolide, and the four analogs (Fig. 1) all induced tubulin assembly in the absence of GTP that is normally required for microtubule assembly (Fig. 2). The microtubules formed in the presence of Taxol, (+)-discodermolide, and the analogs were all stable against calcium-induced depolymerization (data not shown).

Two distinct observations were made. First, the extents of polymerization for (+)-discodermolide, analogs **1** and **2**, and Taxol were essentially the same after 100 min (Fig. 2, curves 1–4). Analogs **3** and **4** demonstrated reduced polymerization, attaining approximately 50% of the level of polymerization observed with (+)-discodermolide (Fig. 2, curves 5 and 6). The proportion of polymerized tubulin for each compound also was determined by removing 200 µl aliquots at the end of the assay, centrifuging at $100\,000 \times g$ for 30 min, and measuring the protein content in the supernatant. By this method, the level of polymerization induced by (+)-discodermolide and analogs **1** and **2** was comparable, whereas analogs **3** and **4** had approximately 50% more protein in the supernatant and hence less polymer in the precipitate (data not shown). Second, the initial slopes (0–5 min) are presented in the inset in Fig. 2. The slope for (+)-discodermolide (curve 1) was assigned a value of 1.0 to which the slopes for the other compounds were compared. The structural analogs (curves 3–6) gave values of 0.26, 0.39, 0.08, and 0.14, respectively; Taxol had a value of 0.28 (curve 2). These data reflect the potent nucleating activity of (+)-discodermolide, and its extreme sensitivity to small modifications in the (+)-discodermolide structure.

2.3. Electron microscopy (EM) reveals differences in the lengths of microtubules formed in the presence of (+)-discodermolide compared to the analogs

The microtubule protein (MTP) from each in vitro assay was examined by EM to confirm that normal microtubules were formed in the presence of the compounds. In all cases, except for the dimethyl sulfoxide (DMSO) control, microtubules were observed (data not shown). As has been noted previously [18], (+)-discodermolide produced much shorter microtubules than those formed in the presence of GTP or Taxol, emphasizing the major effect that (+)-discodermolide has on microtubule nucleation (Fig. 3a–d). Most interesting was the observation that small changes in the (+)-discodermolide structure, such as in analog **1**, resulted in a significant loss of the enhancement of tubulin nucleation (Fig. 3e,f). The microtubules assembled in the presence of (+)-discodermolide were approximately 5-fold, 12-fold, and 4-fold shorter than those formed by analogs **1** and **2**, by analogs **3** and **4**, and by Taxol, respectively (Table 1).

2.4. The drug binding competition assay demonstrates that (+)-discodermolide and the analogs are competitive inhibitors of [^{3}H]Taxol binding

In order to determine the ability of the discodermolide analogs to inhibit the binding of Taxol to preformed microtubules, a drug binding competition assay was performed using [^{3}H]Taxol and purified tubulin. It was found

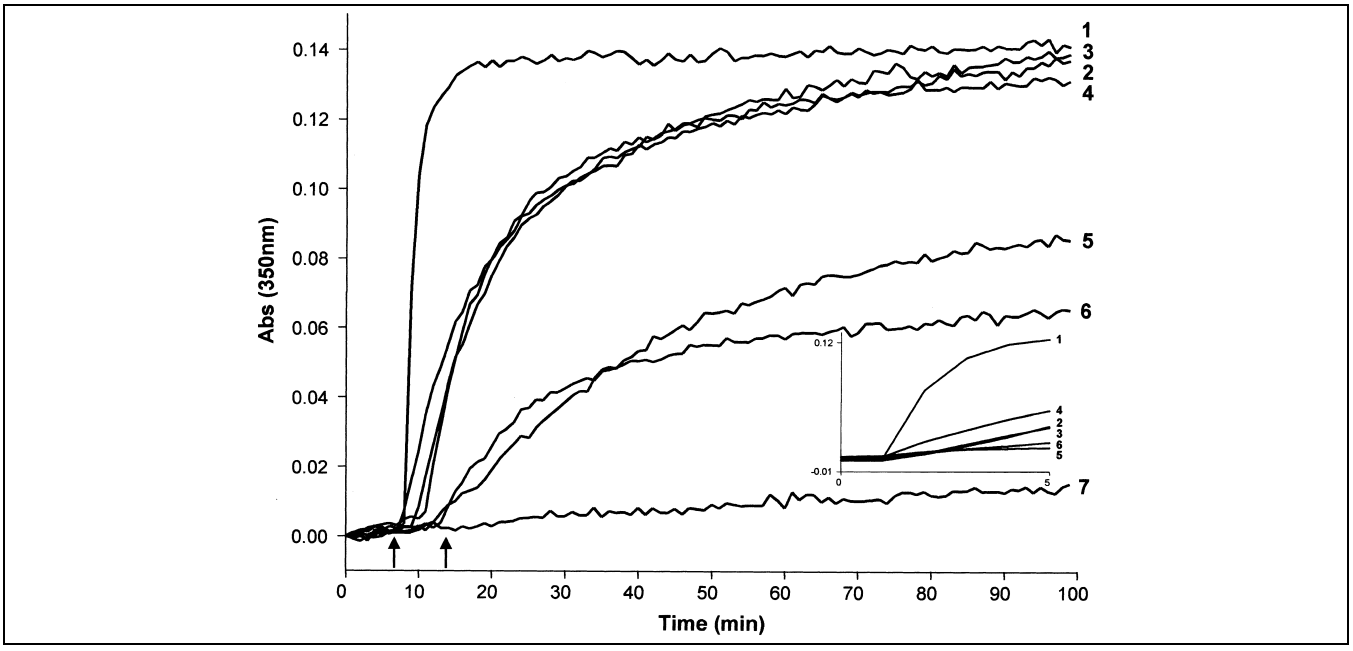

Fig. 2. In vitro activities of Taxol, (+)-discodermolide, and the analogs using a tubulin polymerization assay. MTP was diluted to 1 mg/ml in MES buffer containing 3 M glycerol and the compounds (10 µM) to be evaluated were then added in 1 min intervals (between the arrows) to the MTP incubating at 37°C. The change in absorbance was followed at 350 nm for 100 min. 1, (+)-discodermolide; 2, Taxol; 3, analog **1**; 4, analog **2**; 5, analog **3**; 6, analog **4**; 7, control (DMSO). Inset, initial slope (0–5 min) of Taxol, (+)-discodermolide, and analogs **1–4**.

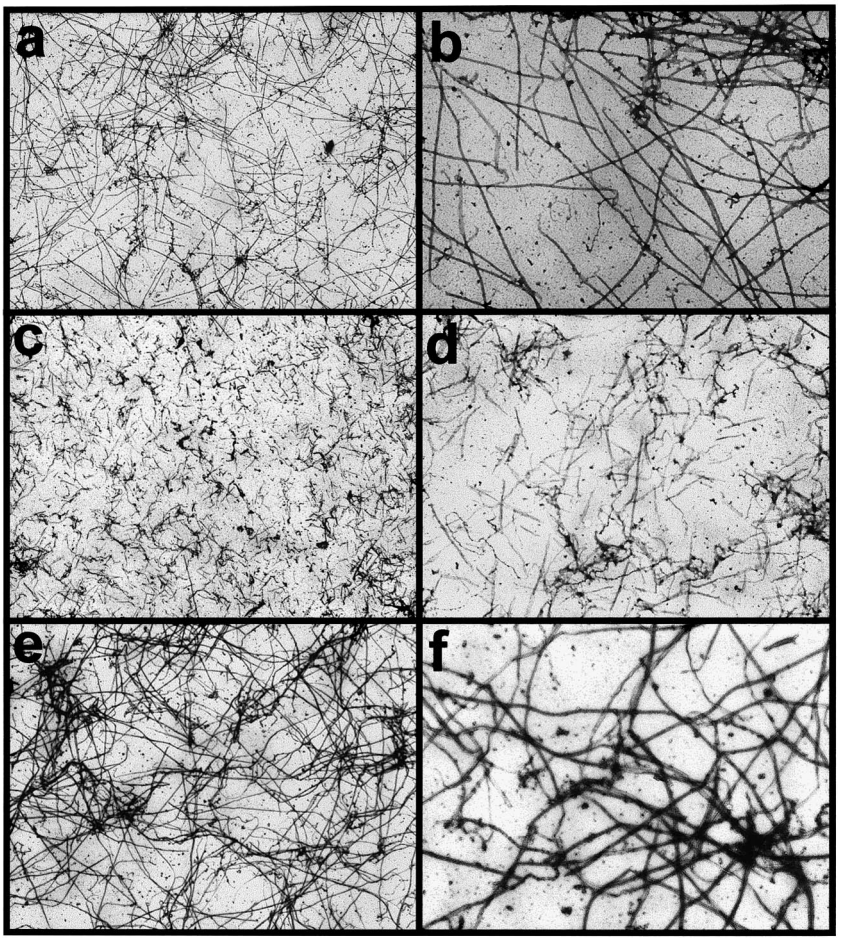

Fig. 3. Electron micrographs of samples from the tubulin polymerization assay demonstrated differences in microtubule length. Aliquots (50 μl) were taken from the cuvettes at the completion of the in vitro assay (100 min) and processed for EM analysis. (a,b) Taxol, (c,d) (+)-discodermolide, and (e,f) analog **1**. (a,c,e) ×5000 magnification; (b,d,f) ×20 000 magnification.

that each of the drugs was a competitive inhibitor of the binding of [^{3}H]Taxol to the preformed microtubules. At 1 μM, Taxol, (+)-discodermolide, and analogs **1–3** exhibited very similar inhibition, whereas analog **4** was essentially inactive in displacing [^{3}H]Taxol binding (Fig. 4). Taxol and (+)-discodermolide, at 10 μM, inhibited the binding of [^{3}H]Taxol by approximately 45%. The discodermolide analogs demonstrated between 5 and 40% inhibition. The differences between the drugs were apparent at 100 μM with (+)-discodermolide displaying almost 95% inhibition and Taxol with 80% inhibition. Analog **1** exhibited greater than 90% inhibition. Discodermolide analogs **2–4** demonstrated a range of between 45 and 65% inhibition. The relative binding affinities of the molecules, the EC_{50} and EC_{75} (inset in Fig. 4), were calculated from the plot of competitive inhibition of [^{3}H]Taxol binding (Fig. 4).

Table 1
A comparison of microtubule lengths after assembly with Taxol, discodermolide, and analogs

Compound	Average polymer length (μm)
Taxol	3.3 ± 1.2[a]
Discodermolide	0.78 ± 0.3
1	5.1 ± 2.2
2	3.0 ± 1.0
3	9.3 ± 4.0
4	9.8 ± 4.9

[a] Mean ± S.E.M.

2.5. *(+)-Discodermolide and the analogs prove active in human A549 and SKOV3 carcinoma cell lines*

(+)-Discodermolide and the analogs all inhibited the proliferation of A549 cells, but to different extents. Taxol and analog **1** shared similar IC_{50} values, followed by (+)-discodermolide (Table 2). Analog **2**, which was as active in vitro as the above compounds, was approximately 2-fold less cytotoxic than (+)-discodermolide. Although analogs **3** and **4** both shared similar in vitro activity, analog **3** had an approximately 3-fold decrease in cytotoxicity while analog **4** had a 128-fold decrease compared to (+)-discodermolide. Similar results were obtained with SKOV3 cells, although (+)-discodermolide was approximately 8-fold less active in this cell line compared to A549 cells

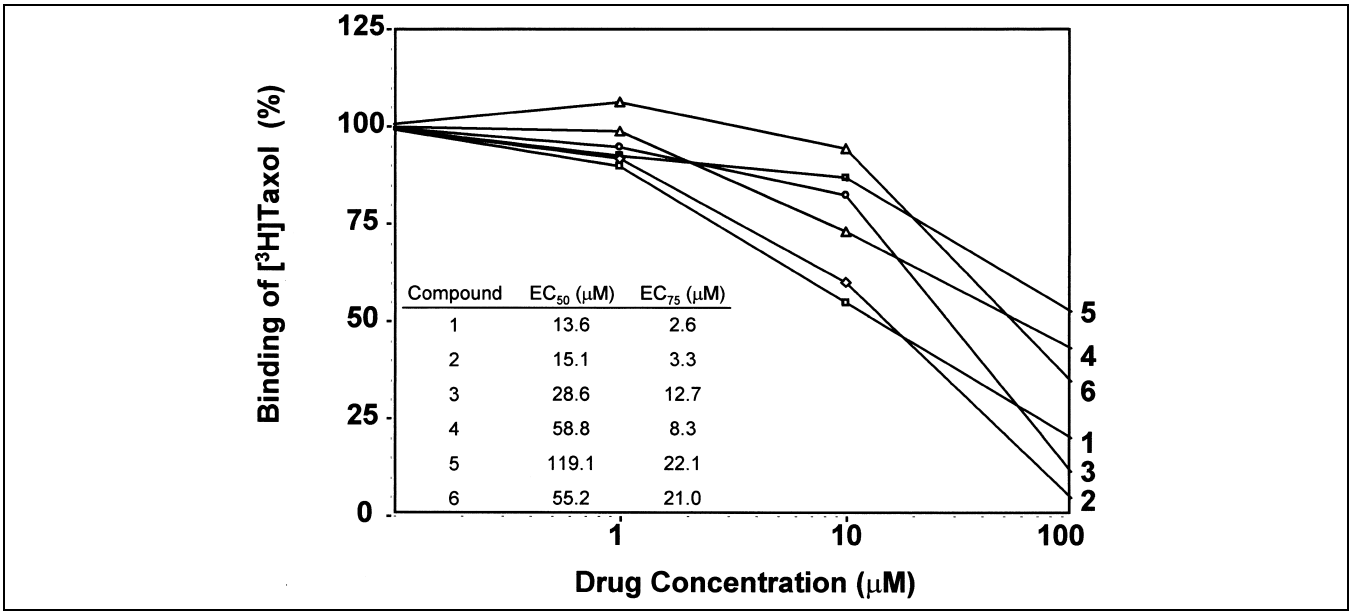

Fig. 4. (+)-Discodermolide and the analogs competitively inhibit the binding of [^{3}H]Taxol to microtubules. Preformed microtubules were incubated with 100 nM [^{3}H]Taxol and competing drugs at 37°C for 30 min. Microtubules were collected by ultracentrifugation and the radioactivity was determined using a liquid scintillation counter. 1, Taxol; 2, (+)-discodermolide; 3, analog **1**; 4, analog **2**; 5, analog **3**; 6, analog **4**. Inset, EC_{50} and EC_{75} values for Taxol, (+)-discodermolide, and analogs **1–4**.

(Table 2). Taxol and analog **1** had comparable IC_{50} values, while discodermolide, analog **2**, and analog **3** were less cytotoxic. As seen in A549 cells, analog **4** displayed the greatest decrease in cytotoxicity.

2.6. A549 cells arrest in mitosis and display microtubule bundles in the presence of (+)-discodermolide and the analogs

Under control conditions, A549 cells exhibited a normal cell cycle profile, microtubule cytoskeleton, and DNA staining (Figs. 5a and 6a). Analysis by flow cytometry indicated that A549 cells are blocked in the G2/M phase of the cell cycle after exposure to a cytotoxic concentration (25 nM) of (+)-discodermolide (Fig. 5b). An increase in the hypodiploid population of cells also was observed, most likely indicating apoptosis. Microtubule bundles and condensed nuclear DNA appeared at this concentra-

Table 2
Cytotoxicity of Taxol, discodermolide, and its analogs in the human A549 and SKOV3 cell lines

Compound	IC_{50} (nM)[a]	
	A549	SKOV3
Taxol	1.4 ± 0.5[b]	3.3 ± 0.5
Discodermolide	3.8 ± 0.6	31.3 ± 6.8
1	1.8 ± 0.1	6.1 ± 3.7
2	7.8 ± 3.3	22.0 ± 10.6
3	11.4 ± 3.2	31.3 ± 16.5
4	485.0 ± 6.4	353.0 ± 0.8

[a] IC_{50}, drug concentration that inhibits cell division by 50% after 72 h.
[b] Mean ± S.E.M.

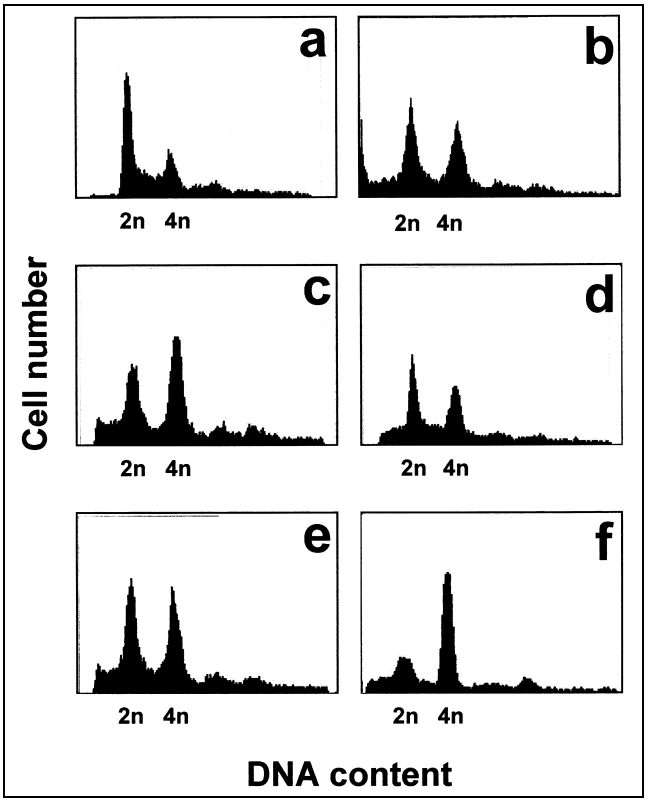

Fig. 5. (+)-Discodermolide and the analogs all induce mitotic arrest in A549 cells. Cells were incubated with different compounds for 24 h, fixed, stained with propidium iodide, and analyzed by flow cytometry. (a) Control (DMSO), (b) (+)-discodermolide (25 nM), (c) analog **1** (10 nM), (d) analog **2** (25 nM), (e) analog **3** (50 nM), and (f) analog **4** (10 μM).

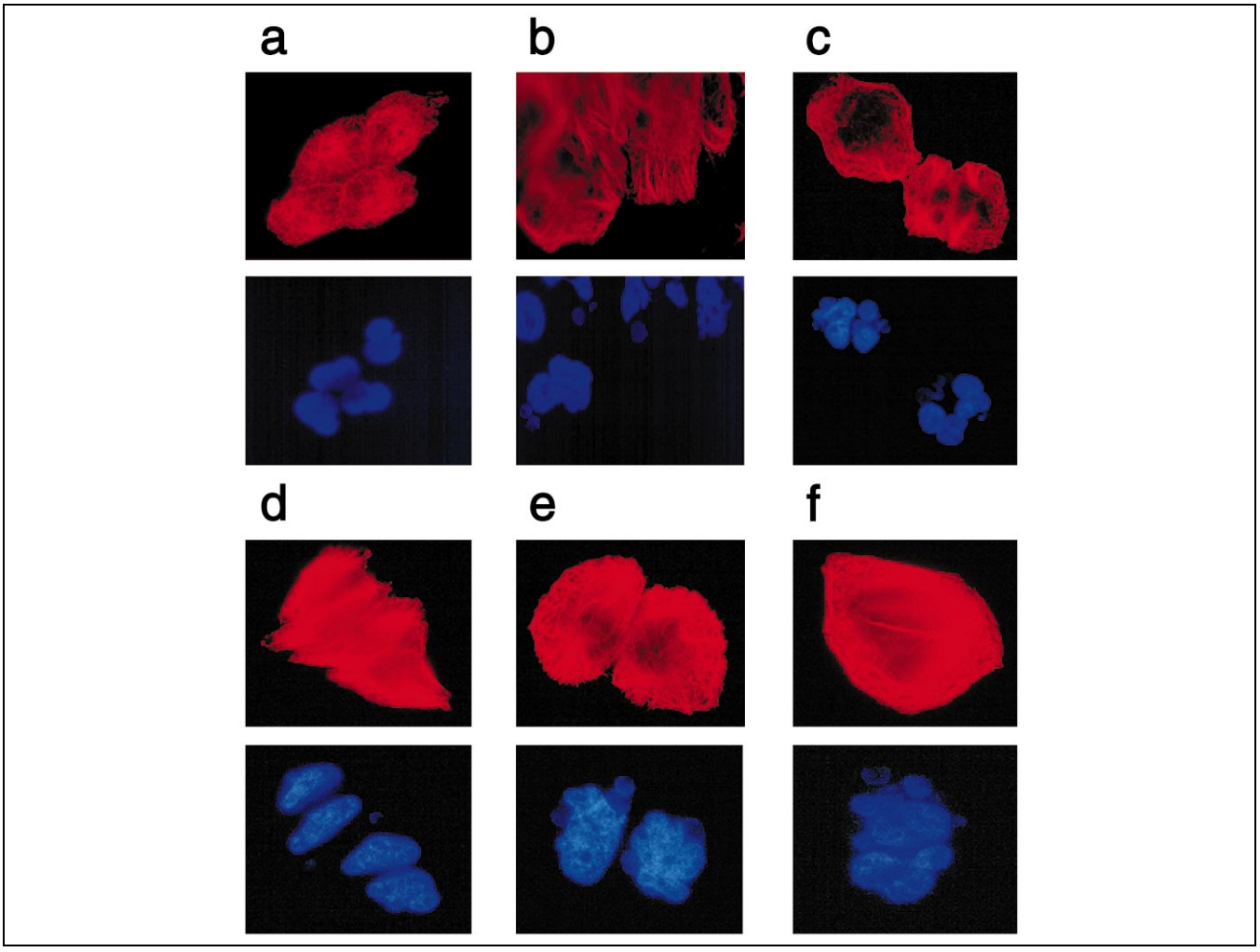

Fig. 6. Microtubule bundle formation is observed in the presence of cytotoxic concentrations of (+)-discodermolide and the analogs. For immunofluorescence studies, A549 cells were grown on coverslips and treated with the different compounds for 24 h. Cells were then permeabilized, fixed, and stained with α-tubulin primary antibody, Cy3 secondary antibody and Hoechst DNA stain. (a) Control (DMSO), (b) (+)-discodermolide (25 nM), (c) analog **1** (10 nM), (d) analog **2** (25 nM), (e) analog **3** (50 nM), and (f) analog **4** (10 μM).

tion as shown by immunofluorescence (Fig. 6b). This effect also was seen at concentrations above 25 nM, but not at concentrations below 12 nM (data not shown). Bundle formations observed with (+)-discodermolide were distinctly different from those noted with Taxol. In the presence of (+)-discodermolide, microtubule bundles were seen at the periphery of the cells, in contrast to Taxol, where the bundles were present throughout the cells (data not shown). At different cytotoxic concentrations, the discodermolide analogs caused arrest in the G2/M phase of the cell cycle and induced microtubule bundling and DNA condensation (Figs. 5c–f and 6c–f).

2.7. *(+)-Discodermolide and Taxol fit within the same binding pocket in the β-tubulin model*

Both the crystal and recent solution structures of (+)-discodermolide [46] demonstrated that the molecule arranges the C1–C19 region into a U-shaped conformation bringing the δ-lactone and the C19 side chain in close proximity. When overlaid with Taxol, the backbone of (+)-discodermolide mimics the northern portion of the taxane ring. The δ-lactone and the C19 side chain of (+)-discodermolide correspond to the C13 and C2 side chains of Taxol. However, the position of the δ-lactone and the C19 side chain with respect to the side chains of Taxol cannot be determined at this point (Fig. 7a,b). Since the crystal/solution structure of the (+)-discodermolide molecule can fit into the Taxol binding pocket within β-tubulin in either of two orientations, two models have been proposed (Fig. 7c,d).

In model I (Fig. 7c), the C19 side chain of (+)-discodermolide, like the C2 benzoyl group of Taxol, binds in a pocket formed by His227 and Asp224 and both side chains are approximately 2–3 Å away from these amino acids. A comparison of the structures of Taxol and Taxotere, both used for the treatment of human carcinomas [1], shows a replacement at the C10 position (hydroxyl

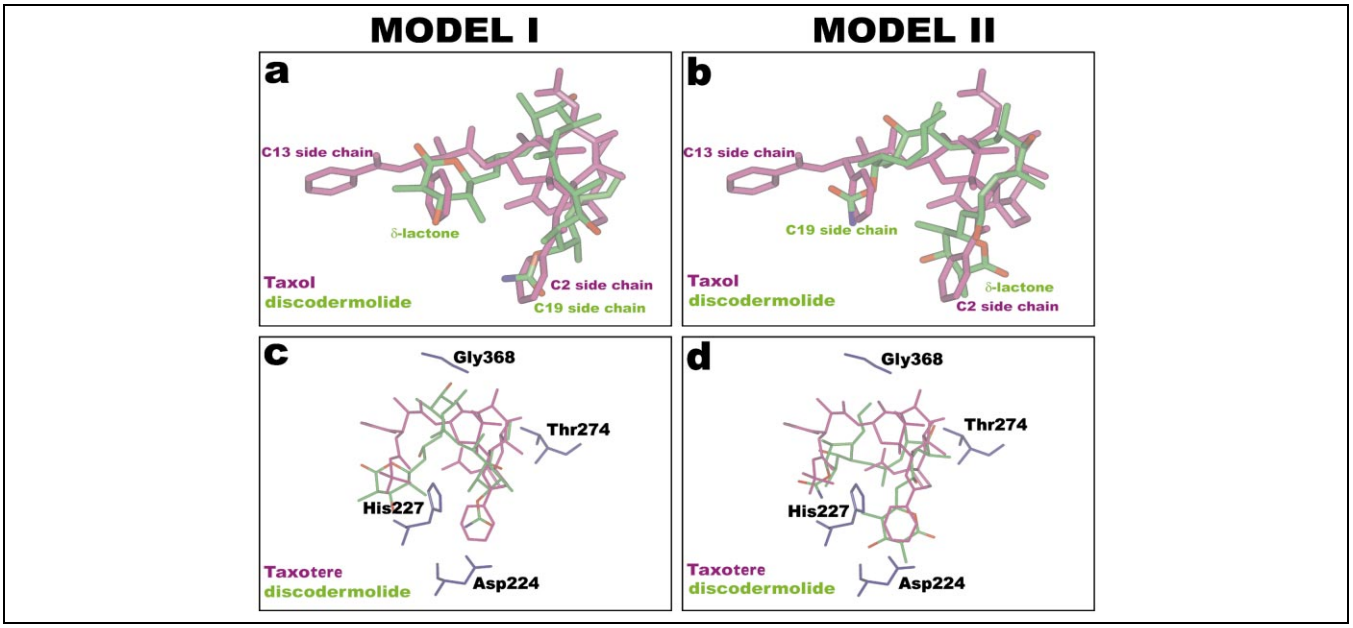

Fig. 7. (+)-Discodermolide mimics Taxol and binds into a pocket formed by Gly368, Thr274, His227 and Asp224 in β-tubulin. (a) Model I: the folded U-shaped backbone of (+)-discodermolide matches with the taxane ring of Taxol and the C19 side chain of (+)-discodermolide mimics the C2 side chain of Taxol, while the δ-lactone of (+)-discodermolide emulates the C13 side chain of Taxol (pink: Taxol; green: (+)-discodermolide). (b) Model II: the δ-lactone of (+)-discodermolide matches with the C2 side chain of Taxol and the C19 side chain of (+)-discodermolide mimics the C13 side chain of Taxol. (c) Model I: (+)-discodermolide, in the first orientation as seen in (a), fits into the Taxol binding pocket formed by Gly368, Thr274, His227, and Asp224 of β-tubulin (pink: Taxotere; green: (+)-discodermolide; β-tubulin amino acids highlighted in purple). (d) Model II: (+)-discodermolide, in the second orientation as seen in (b), also fits into the Taxol binding pocket within β-tubulin.

group) and the C3′ position on the C13 side chain (tertiary butyl group) in the Taxotere structure (Fig. 1). If Taxol is replaced by Taxotere, modeling studies revealed a much better fit between the δ-lactone of (+)-discodermolide and the C13 side chain of Taxotere. The C4 methyl group of the δ-lactone is approximately 1 Å away from His227, while the tertiary butyl group is approximately 2.5 Å in distance from His227. The C11 hydroxyl group of (+)-discodermolide matches with the C10 acetyl group of Taxol and both groups are approximately 2.5 Å from Gly368. The final contact with Thr274 is made between C24 of (+)-discodermolide and the C7 hydroxyl group of Taxol, both approximately 2.8 Å from Thr274.

In model II (Fig. 7d), the δ-lactone fits into the binding pocket formed by His227 and Asp224, in a similar manner to the C2 benzoyl group of Taxol. The C4 methyl group of the δ-lactone is approximately 1 Å from His227 and 3 Å from Asp224. The C19 side chain of (+)-discodermolide is found near His227 (approximately 5 Å away), similar to the C3′ tertiary butyl group of Taxotere. The C7 hydroxyl group of Taxol matches with the C10 methyl group of (+)-discodermolide, making contact with Thr274. The C10 methyl group is approximately 2.5 Å from the hydroxyl group of Thr274. The Gly368 contact is made between the C12 methyl group (4 Å) and C24 (1.3 Å) of (+)-discodermolide, in a similar manner to that of the C10 acetyl group of Taxol.

The four discodermolide analogs also were modeled in place of (+)-discodermolide in the β-tubulin structure (data not shown). In model I, analogs **1**, **2**, and **3** do not lose any important contacts with β-tubulin since the positions on the molecule that have been modified are not in contact with what appear to be important residues responsible for drug binding. In analog **1**, the C4 methyl group is in contact with His227 of β-tubulin while the C3 hydroxyl group that was removed did not make any significant contacts. The C14 methyl group of analog **2** and the C7 hydroxyl group of analog **3** both are present in an open area within the drug binding pocket. Analog **3** may be slightly less cytotoxic due to the additive effect of removing both the C3 and C7 hydroxyl groups. A comparison of (+)-discodermolide with analog **4**, which has the altered olefin geometry at C8, not surprisingly demonstrated a dramatic change in the overall conformation. In particular, the δ-lactone of analog **4** would lose binding to His227 when placed into the β-tubulin model and would no longer mimic the tertiary butyl group of Taxotere. Instead, the δ-lactone is shifted, losing contact with His227 and making new contacts with β-tubulin, possibly at Leu273. New interactions may explain why this analog, although less cytotoxic than analogs **1–3**, retains some activity. In model II, analogs **1** and **2** again do not lose the necessary contacts within the drug binding pocket. In contrast, analog **3** would lose a specific contact with Arg276 that appears to be important for binding and activity, and analog **4** would lose all contacts, including those with His227 and Asp224. Moreover, the δ-lactone of analog **4** would now point out of the binding pocket

towards the lumen of the microtubule structure. Since analog **3** does not demonstrate a significant decrease in cytotoxicity and analog **4** retains activity in the high nM range, model II is not supported. Therefore, we favor model I as the orientation of (+)-discodermolide within the β-tubulin structure. The availability of additional synthetic analogs should increase our knowledge of the interaction between (+)-discodermolide and microtubules.

3. Discussion

In this report, we have compared the activity of (+)-discodermolide with four structural analogs. Our results suggest a common pharmacophore model for Taxol and (+)-discodermolide. The in vitro studies demonstrated that (+)-discodermolide and the structural analogs induced tubulin assembly in the absence of GTP and that the microtubules formed were stable under depolymerizing conditions. The initial rate of tubulin polymerization in the presence of (+)-discodermolide was dramatically different compared to the analogs. Even a single change to the (+)-discodermolide structure reduced the potent nucleating activity of the analogs, presumably due to a loss of a specific contact between the analogs and β-tubulin that must be necessary for enhanced initiation of tubulin polymerization. It has been noted that Taxol does not possess the same ability to hypernucleate tubulin assembly as (+)-discodermolide [10], and that (+)-discodermolide produced shorter microtubules than Taxol [18]. EM revealed that the microtubules formed in the presence of (+)-discodermolide were significantly shorter than those produced by the analogs and by Taxol. In addition, (+)-discodermolide and the analogs inhibited the binding of [^{3}H]Taxol to microtubules, but to different extents. (+)-Discodermolide and the analogs also were cytotoxic to human A549 lung and SKOV3 ovarian carcinoma cells. In both cell lines, analog **4** displayed the most dramatic decrease in cytotoxicity. Although analog **4** is only 50% less active in vitro, in A549 and SKOV3 cells analog **4** exhibited a much more significant decrease in cytotoxicity compared to the other analogs. This effect could be due to a decrease in accessibility to the β-tubulin binding sites in cells, compared to in vitro conditions with purified tubulin. The results from the three different assays, the in vitro tubulin assembly assay, the [^{3}H]Taxol binding competition assay, and the cytotoxicity studies, indicated that Taxol, (+)-discodermolide, and analog **1** are the most active compounds whereas analogs **3** and **4**, especially analog **4**, are the least active. The results obtained from calculating the relative binding affinities have suggested that the interaction of the drug with the microtubule is not always correlative with cytotoxicity. It should be noted that the in vitro assembly assay provides information such as the unique nucleating activity of (+)-discodermolide that is not observed in any of the other assays.

The (+)-discodermolide X-ray/solution structure was modeled with Taxol and the overall conformation was found to be similar in both orientations (models I and II) (Fig. 7a,b). The backbone of (+)-discodermolide, as displayed in the crystal/solution conformation, overlaid the northern portion of the taxane ring. Our previous photoaffinity labeling studies and molecular modeling work have suggested that Taxol binds into a pocket formed by Gly368, Thr274, His227, and Asp224 in β-tubulin [15,47]. This information allowed us to suggest that like Taxol, (+)-discodermolide fits into this β-tubulin binding cavity and thereby affects the M-loop of β-tubulin and stabilizes the interactions between adjacent protofilaments [15,48]. This is consistent with the observations that (+)-discodermolide possesses a similar mechanism of action as Taxol and that (+)-discodermolide and Taxol compete for a binding site in β-tubulin [11]. Using this model, (+)-discodermolide was found to fit into the Taxol binding pocket in either of two binding modes (models I and II) (Fig. 7c,d).

The modeling work performed with (+)-discodermolide has shed further light on a common pharmacophore for Taxol, the epothilones, eleutherobin, and (+)-discodermolide. Two elements appear to be required for microtubule-stabilizing activities: a core ring structure similar to the taxane ring of Taxol and a side chain comparable to the C2 benzoyl group of Taxol. The C13 side chain is not an absolute requirement for Taxol-like activity, since 2-*m*-azido baccatin III has activity that is dependent on the substituent at the 2-*meta* position [15]. The macrolide ring of the epothilones, the core ring system of eleutherobin, and the U-shaped backbone of (+)-discodermolide all mimic the taxane ring of Taxol. The thiazole side chain of the epothilones, the C8 methylurocanic acid side chain of eleutherobin, and the C19 side chain of (+)-discodermolide match with the C2 benzoyl group of Taxol. The core structure of these compounds binds in a pocket formed by Gly368, Thr274, His227 and Asp224 in β-tubulin and their side chains fit into a pocket formed by His227 and Asp224 [15].

There are still unresolved issues relating to the activity of (+)-discodermolide. For example, it is not obvious why (+)-discodermolide, compared to the analogs and Taxol, is extremely competent at initiating tubulin polymerization or how this may affect the chemotherapeutic activity of the drug. Also, a lack of cross-resistance to (+)-discodermolide was found in the A549-T12 Taxol-resistant cell line, although the cells were cross-resistant to the epothilones. In addition, (+)-discodermolide was unable to substitute for Taxol in A549-T12 cells that require low concentrations of Taxol for normal growth [19]. In contrast, the epothilones were able to support the growth of A549-T12 cells. This cell line does not have a mutation in class I β-tubulin (L.A. Martello, unpublished observation). Furthermore, epothilone-resistant cells with class I β-tubulin mutations displayed no cross-resistance to (+)-discoder-

molide (P. Giannakakou, personal communication). These results suggest that there are distinct differences between the interaction of Taxol, the epothilones, and (+)-discodermolide with microtubules that may indicate overlapping but not identical binding sites. In comparison to Taxol, (+)-discodermolide may be forming additional or discrete contacts within the β-tubulin structure. It is possible that (+)-discodermolide also may have additional targets within cells that allow it to remain cytotoxic in drug-resistant cell lines that may or may not have β-tubulin mutations.

4. Significance

Discodermolide analogs (**1–4**) were synthesized via a highly efficient, triply convergent approach to (+)-discodermolide and evaluated both in vitro and in human carcinoma cell lines. The analogs were devised not only to simplify the structure of (+)-discodermolide but also the required synthetic strategy, while retaining cytotoxic activity. The SAR studies demonstrated that small changes to the (+)-discodermolide structure resulted in a dramatic decrease in the initiation of tubulin polymerization. Specific modifications made to analogs **3** and **4** also caused a decrease in total tubulin polymerization. In addition, a change in the olefin geometry at C8 in analog **4** produced a significant decrease in cytotoxicity. Molecular modeling studies using the X-ray/solution structure of (+)-discodermolide revealed that the molecule folds into a U-shaped conformation. Two potential binding models were possible when the X-ray/solution structure of (+)-discodermolide was docked into the Taxol binding pocket in β-tubulin. Model I, in which the C19 side chain of (+)-discodermolide matches with the C2 benzoyl group of Taxol and the δ-lactone of (+)-discodermolide fits with the C13 side chain of Taxol, is most consistent with the results of the SAR studies. Finally, this report presents important information on the structural requirements of (+)-discodermolide that confer unique activity and potency. Our future goals are to explore further the similarities and differences between Taxol and (+)-discodermolide in order to exploit this knowledge for both the design of new cancer chemotherapeutic drugs and improved treatment regimens.

5. Materials and methods

5.1. Materials

All drugs were dissolved in sterile DMSO and stored at −20°C. MTP was purified by two cycles of temperature-dependent assembly–disassembly from calf brain and stored in liquid nitrogen [49]. The concentration of tubulin in the MTP preparation was approximately 85%.

5.2. Cell culture

The A549 lung carcinoma cell line was maintained as described previously [50]. The SKOV3 ovarian carcinoma cell line was obtained from Dr. V. Ling and was maintained as described previously [32].

5.3. In vitro tubulin polymerization assay

Microtubule polymerization was evaluated by recording the change in turbidity of MTP at 350 nm for 100 min in a spectrophotometer (UVIKON, Research Instruments Int., San Diego, CA, USA) [51]. Purified MTP was diluted in assembly buffer containing 0.1 M MES, 1 mM EGTA, 0.5 mM $MgCl_2$, and 3 M glycerol (pH 6.6) to a final concentration of 1 mg/ml. All compounds were evaluated at a concentration of 10 μM at 37°C in the absence of GTP. The changes in absorption that occurred during the first 5 min were used to plot initial slopes from the linear portion of each curve in order to compare the initial activity of each compound.

5.4. EM

Aliquots (50 μl) were taken from the in vitro polymerization assay at the end of the reaction and placed onto 300-mesh carbon-coated, Formavar-treated copper grids. Samples were then stained with 20 μl of 2% uranyl acetate and viewed with a JEOL model 100CX electron microscope. To determine the lengths of the microtubules, electron micrograph negatives were scanned and then analyzed using IP Lab software. Measurements were performed on negatives at $\times 10\,000$ and $\times 5000$, with a minimum of 50 microtubules measured for each compound.

5.5. Drug binding competition assay

The assay was performed using methods described previously [8,15]. MTP (0.4 mg/ml) was incubated at 37°C with 1 mM GTP and 7.5 nM Taxol for 20 min to induce the assembly of microtubules. One hundred nM [^{3}H]Taxol (specific activity: 19.3 Ci/mmol) and the indicated concentration of the competing agent were added simultaneously to the preformed microtubules. The mixtures were further incubated at 37°C for 30 min to allow binding of [^{3}H]Taxol. Microtubules were collected by ultracentrifugation ($100\,000 \times g$, 1 h, 30°C) and the radioactivity measured using a liquid scintillation counter. The inhibition of binding of [^{3}H]Taxol to microtubules was expressed as a percentage compared to the control (100%). The determination of the relative binding affinities using the percentage of competitive inhibition of [^{3}H]Taxol binding was obtained through linear regression analysis. The effective concentrations that inhibit 50% (EC_{50}) and 75% (EC_{75}) of [^{3}H]Taxol binding were determined.

5.6. Cytotoxicity assays

A549 cells were seeded in triplicate at a density of 1×10^4 cells/ml in 6-well plates and allowed to attach for 24 h. After incubation with various drug concentrations for 72 h, adherent cells were trypsinized and counted (Coulter Counter model Z1; Coulter Corp., Miami, FL, USA), and the IC_{50} was determined. SKOV3 cells were seeded at a density of 2×10^4 cells/ml and the above procedure followed.

5.7. Flow cytometry

A549 cells were prepared for flow cytometry as described previously except that drug treatment was for 24 h [19].

5.8. Immunofluorescence

A549 cells were prepared for immunofluorescence as described previously [19]. In addition, cells were stained with Hoechst solution (Sigma; 1:2.5 dilution) for 15 min after the secondary antibody wash. Slides were analyzed using a Zeiss Axiophot microscope (rhodamine and DAPI filters) at $\times 100$ magnification.

5.9. Molecular modeling

Molecular modeling studies were performed using the Insight II software (Molecular Simulations Inc.). The α,β-tubulin structure was taken from Nogales et al. (PDB code: 1TUB) [52]. The coordinates for the Taxol X-ray structure were developed by Mastropaolo et al. [53] and the Taxotere X-ray structure coordinates were acquired from Gueritte-Voegelein et al. [54]. The coordinates for (+)-discodermolide, obtained from Gunasekera et al., required sign inversion to conform to the correct absolute stereochemistry [55].

Acknowledgements

We thank Michael Cammer and Frank Macaluso of the Analytical Imaging Facility for assistance with the microtubule measurements and Dr. Fred Brewer for the use of computers for the modeling studies (AECOM). The work at AECOM was supported in part by USPHS Grants CA 39821 and CA 77263 (S.B.H.), Cancer Core Support Grant CA 13330, and the National Institute of General Medical Sciences Training Program in Pharmacological Sciences Grant 5T32 GM07260 (L.A.M.). At the University of Pennsylvania, work was supported by the Department of the Army through Grant DAMD 17-00-1-0404 and Novartis Pharmaceutical Company.

References

[1] E.K. Rowinsky, The development and clinical utility of the taxane class of antimicrotubule chemotherapy agents, Annu. Rev. Med. 48 (1997) 353–374.
[2] P.B. Schiff, J. Fant, S.B. Horwitz, Promotion of microtubule assembly in vitro by Taxol, Nature (Lond.) 277 (1979) 665–667.
[3] P.B. Schiff, S.B. Horwitz, Taxol stabilizes microtubules in mouse fibroblast cells, Proc. Natl. Acad. Sci. USA 77 (1980) 1561–1565.
[4] M.A. Jordan, K. Wendell, S. Gardiner, W.B. Derry, H. Copp, L. Wilson, Mitotic block induced in HeLa cells by low concentrations of paclitaxel (Taxol) results in abnormal mitotic exit and apoptotic cell death, Cancer Res. 56 (1996) 816–825.
[5] K. Torres, S.B. Horwitz, Mechanisms of Taxol-induced cell death are concentration dependent, Cancer Res. 58 (1998) 3620–3626.
[6] M.A. Jordan, R.J. Toso, D. Thrower, L. Wilson, Mechanism of mitotic block and inhibition of cell proliferation by Taxol at low concentrations, Proc. Natl. Acad. Sci. USA 90 (1993) 9552–9556.
[7] W.B. Derry, L. Wilson, M.A. Jordan, Substoichiometric binding of Taxol suppresses microtubule dynamics, Biochemistry 34 (1995) 2203–2211.
[8] D.M. Bollag, P.A. McQueney, J. Zhu, O. Hensens, L. Koupal, J. Liesch, M. Goetz, E. Lazarides, C.M. Woods, Epothilones, a new class of microtubule-stabilizing agents with a Taxol-like mechanism of action, Cancer Res. 55 (1995) 2325–2333.
[9] T. Lindel, P.R. Jensen, W. Fenical, B.H. Long, A.M. Casazza, J. Carboni, C.R. Fairchild, Eleutherobin, a new cytotoxin that mimics Paclitaxel (Taxol) by stabilizing microtubules, J. Am. Chem. Soc. 119 (1997) 8744–8745.
[10] E. Ter Haar, R.J. Kowalski, E. Hamel, C.M. Lin, R.E. Longley, S.P. Gunasekera, H.S. Rosenkranz, B.W. Day, Discodermolide, a cytotoxic marine agent that stabilizes microtubules more potently than Taxol, Biochemistry 35 (1996) 243–250.
[11] D.T. Hung, J. Chen, S.L. Schreiber, (+)-Discodermolide binds to microtubules in stoichiometric ratio to tubulin dimers, blocks taxol binding and results in mitotic arrest, Chem. Biol. 3 (1996) 287–293.
[12] J.D. Winkler, P.H. Axelsen, A model for the Taxol (Paclitaxel)/epothilone pharmacophore, Bioorg. Med. Chem. Lett. 6 (1996) 2963–2966.
[13] I. Ojima, S. Chakravarty, T. Inoue, S. Lin, L. He, S.B. Horwitz, S.D. Kuduk, S.J. Danishefsky, A common pharmacophore for cytotoxic natural products that stabilize microtubules, Proc. Natl. Acad. Sci. USA 96 (1999) 4256–4261.
[14] M. Wang, X. Xia, Y. Kim, D. Hwang, J.M. Jansen, M. Botta, D.C. Liotta, J.P. Snyder, A unified and quantitative receptor model for the microtubule binding of Paclitaxel and epothilone, Org. Lett. 1 (1999) 43–46.
[15] L. He, P.G. Jagtap, D.G.I. Kingston, H.-J. Shen, G.A. Orr, S.B. Horwitz, A common pharmacophore for Taxol and the epothilones based on the biological activity of a taxane molecule lacking a C-13 side chain, Biochemistry 39 (2000) 3972–3978.
[16] P. Giannakakou, R. Gussio, E. Nogales, K.H. Downing, D. Zaharevitz, B. Bollbuck, G. Poy, D. Sackett, K.C. Nicolaou, T. Fojo, A common pharmacophore for epothilone and taxanes: molecular basis for drug resistance conferred by tubulin mutations in human cancer cells, Proc. Natl. Acad. Sci. USA 97 (2000) 2904–2909.
[17] R.E. Longley, S.P. Gunasekera, D. Faherty, J. McLane, F. Dumont, Immunosuppression by discodermolide, Ann. N.Y. Acad. Sci. 696 (1993) 94–107.
[18] R.J. Kowalski, P. Giannakakou, S.P. Gunasekera, R.E. Longley, B.W. Day, E. Hamel, The microtubule-stabilizing agent discodermolide competitively inhibits the binding of Paclitaxel (Taxol) to tubulin polymers, enhances tubulin nucleation reactions more potently than Paclitaxel, and inhibits the growth of Paclitaxel-resistant cells, Mol. Pharmacol. 52 (1997) 613–622.
[19] L.A. Martello, H.M. McDaid, D. Regl, C.-P.H. Yang, D. Meng, T.R.R. Pettus, M.D. Kaufman, H. Arimoto, S.J. Danishefsky, A.B. Smith III, S.B. Horwitz, Taxol and discodermolide represent a synergistic drug combination in human carcinoma cell lines, Clin. Cancer Res. 6 (2000) 1978–1987.
[20] J.B. Nerenberg, D.T. Hung, P.K. Somers, S.L. Schreiber, Total synthesis of the immunosuppressive agent (−)-discodermolide, J. Am. Chem. Soc. 115 (1993) 12621–12622.
[21] A.B. Smith III, Y. Qiu, D.R. Jones, K. Kobayashi, Total synthesis of (−)-discodermolide, J. Am. Chem. Soc. 117 (1995) 12011–12012.
[22] S.S. Harried, G. Yang, M.A. Strawn, D.C. Myles, Total synthesis of (−)-discodermolide: an application of a chelation-controlled alkylation reaction, J. Org. Chem. 62 (1997) 6098–6099.
[23] J.A. Marshall, B.A. Johns, Total synthesis of (+)-discodermolide, J. Org. Chem. 63 (1998) 7885–7892.
[24] D.P. Halstead, Total synthesis of (+)-miyakolide, (−)-discodermolide, and (+)-discodermolide, Ph.D. thesis, Harvard University, Cambridge, 1998, pp. 1–199.
[25] A.B. Smith III, M.D. Kaufman, T.J. Beauchamp, M.J. LaMarche, H.

Arimoto, Gram-scale synthesis of (+)-discodermolide, Org. Lett. 1 (1999) 1823–1826.
[26] I. Paterson, G.J. Florence, K. Gerlach, J.P. Scott, Total synthesis of the antimicrotubule agent (+)-discodermolide using boron-mediated aldol reactions of chiral ketones, Angew. Chem. Int. Ed. 39 (2000) 377–380.
[27] D.T. Hung, J.B. Nerenberg, S.L. Schreiber, Syntheses of discodermolides useful for investigating microtubule binding and stabilization, J. Am. Chem. Soc. 118 (1996) 11054–11080.
[28] I. Paterson, G.J. Florence, Synthesis of (+)-discodermolide and analogues by control of asymmetric induction in aldol reactions of gamma-chiral (*Z*)-enals, Tetrahedron Lett. 41 (2000) 6935–6939.
[29] D. Kingston, Recent advances in the chemistry and structure–activity relationships of paclitaxel, in: G.I. Georg, T.T. Chen, I. Ojima, D.M. Vyas (Eds.), Taxane Anticancer Agents: Basic Science and Current Status, American Chemical Society, Washington, DC, 1995, pp. 203–216.
[30] D.-S. Su, A. Balog, D. Meng, P. Bertinato, S.J. Danishefsky, Y.-H. Zheng, T.-C. Chou, L. He, S.B. Horwitz, Structure–activity relationships of the epothilones and the first in vivo comparison with Paclitaxel, Angew. Chem. Int. Ed. Engl. 36 (1997) 2093–2096.
[31] K.C. Nicolaou, F. Roschangar, D. Vourloumis, Chemical biology of epothilones, Angew. Chem. Int. Ed. 37 (1998) 2014–2045.
[32] H.M. McDaid, S.K. Bhattacharya, X.-T. Chen, L. He, H.-J. Shen, C.E. Gutteridge, S.B. Horwitz, S.J. Danishefsky, Structure–activity profiles of eleutherobin analogs and their cross-resistance in Taxol-resistant cell lines, Cancer Chemother. Pharmacol. 44 (1999) 131–137.
[33] A.B. Smith III, T.J. Beauchamp, M.J. LaMarche, M.D. Kaufman, Y. Qiu, H. Arimoto, D.R. Jones, K. Kobayashi, Evolution of a gram-scale synthesis of (+)-discodermolide, J. Am. Chem. Soc. 122 (2000) 8654–8664.
[34] P. Kocovsky, Carbamates: a method of synthesis and some synthetic applications, Tetrahedron Lett. 27 (1986) 5521–5524.
[35] D.A. Evans, G.C. Fu, A.H. Hoveyda, Rhodium (I) and iridium (I)-catalyzed hydroboration reactions: scope and synthetic applications, J. Am. Chem. Soc. 114 (1992) 6671–6679.
[36] J.R. Parikh, W.v.E. Doering, Sulfur trioxide in the oxidation of alcohols by dimethyl sulfoxide, J. Am. Chem. Soc. 89 (1967) 5505–5507.
[37] G. Stork, K. Zhao, A stereoselective synthesis of (*Z*)-1-iodo-1-alkenes, Tetrahedron Lett. 30 (1989) 2173–2174.
[38] E. Negishi, L.F. Valente, M. Kobayashi, Palladium-catalyzed cross-coupling reaction of homoallylic or homopropargylic organozincs with alkenyl halides as a new selective route to 1,5-dienes and 1,5-enynes, J. Am. Chem. Soc. 102 (1980) 3298–3299.
[39] S. Takano, M. Akiyama, S. Sato, K. Ogasawara, A facile cleavage of benzylidene acetals with diisobutylaluminum hydride, Chem. Lett. 10 (1983) 1593–1596.
[40] D.B. Dess, J.C. Martin, A useful 12-1-5 triacetoxyperiodinane (the Dess–Martin periodinane) for the selective oxidation of primary or secondary alcohols and a variety of related 12-1-5 species, J. Am. Chem. Soc. 113 (1991) 7277–7287.
[41] Y. Ikeda, J. Ukai, N. Ikeda, H. Yamamoto, Stereoselective synthesis of (*Z*)- and (*E*)-1,3-alkadienes from aldehydes using organotitanium and lithium reagents, Tetrahedron 43 (1987) 723–730.
[42] R.K. Boeckman Jr., J.C. Potenza, Catecholboron halides: mild and selective reagents for cleavage of common protecting groups, Tetrahedron Lett. 26 (1985) 1411–1414.
[43] E.J. Corey, S.G. Pyne, W.-G. Su, Total synthesis of leukotriene B5, Tetrahedron Lett. 24 (1983) 4883–4886.
[44] P.J. Garegg, B. Samuelsson, Novel reagent system for converting a hydroxy-group into an iodo-group in carbohydrates with inversion of configuration. Part 2, J. Chem. Soc. 1 (1980) 2866–2869.
[45] F. Gaskin, C.R. Cantor, M.L. Shelanski, Turbidimetric studies of the in vitro assembly and disassembly of porcine neurotubules, J. Mol. Biol. 89 (1974) 737–758.
[46] A.B.I. Smith III, M.J. LaMarche, M. Falcone-Hindley, The solution structure of (+)-discodermolide, Org. Lett. 5 (2001) 695–698.
[47] S. Rao, L. He, S. Chakravarty, I. Ojima, G.A. Orr, S.B. Horwitz, Characterization of the Taxol binding site on the microtubule. Identification of Arg(282) in β-tubulin as the site of photoincorporation of a 7-benzophenone analogue of Taxol, J. Biol. Chem. 274 (1999) 37990–37994.
[48] E. Nogales, M. Whittaker, R.A. Milligan, K.H. Downing, High-resolution model of the microtubule, Cell 96 (1999) 79–88.
[49] R.C. Weisenberg, Microtubule formation in vitro in solutions containing low calcium concentrations, Science 177 (1972) 1104–1105.
[50] M. Kavallaris, D.Y.-S. Kuo, C.A. Burkhart, D.L. Regl, M.D. Norris, M. Haber, S.B. Horwitz, Taxol-resistant epithelial ovarian tumors are associated with altered expression of specific β-tubulin isotypes, J. Clin. Invest. 100 (1997) 1282–1293.
[51] M.L. Shelanski, F. Gaskin, C.R. Cantor, Microtubule assembly in the absence of added nucleotides, Proc. Natl. Acad. Sci. USA 70 (1973) 765–768.
[52] E. Nogales, S.G. Wolf, K.H. Downing, Structure of the αβ tubulin dimer by electron crystallography, Nature 391 (1998) 199–203.
[53] D. Mastropaolo, A. Camerman, Y. Luo, G.D. Brayer, N. Camerman, Crystal and molecular structure of Paclitaxel (Taxol), Proc. Natl. Acad. Sci. USA 92 (1995) 6920–6924.
[54] F. Gueritte-Voegelein, D. Guenard, L. Mangatal, P. Potier, J. Guilhem, M. Cesario, C. Pascard, Structure of a synthetic taxol precursor: *N-tert*-butoxycarbonyl-10-deacetyl-*N*-debenzoyltaxol, Acta Crystallogr. C46 (1990) 781–784.
[55] S.P. Gunasekera, M. Gunasekera, R.E. Longley, Discodermolide: A new bioactive polyhydroxylated lactone from the marine sponge *Discodermia dissoluta*, J. Org. Chem. 55 (1990) 4912–4915.